Miocene Tectonic Evolution from Dextral-Slip Thrusting to Extension in the Nyainqêntanglha Region of the Tibetan Plateau

WU Zhenhan[1,*], Patrick J. BAROSH[2], ZHAO Xun[3], WU Zhonghai[1], HU Daogong[1] and LIU Qisheng[1]

1 *Institute of Geomechanics, Chinese Academy of Geological Sciences, Beijing 100081, China*

2 *P. J. Barosh 103 Aaron Avenue, Bristol, RI 02809, USA*

3 *Chinese Academy of Geological Sciences, Beijing 100037, China*

Abstract: Dextral-slip in the Nyainqêntanglha region of Tibet resulted in oblique underthrusting and granite generation in the Early to Middle Miocene, but by the end of the epoch uplift and extensional faulting dominated. The east-west dextral-slip Gangdise fault system merges eastward into the northeast-trending, southeast-dipping Nyainqêntanglha thrust system that swings eastward farther north into the dextral-slip North Damxung shear zone and Jiali faults. These faults were took shape by the Early Miocene, and the large Nyainqêntanglha granitic batholith formed along the thrust system in 18.3-11.0 Ma as the western block drove under the eastern one. The dextral-slip movement ended at ~11 Ma and the batholith rose, as marked by gravitational shearing at 8.6–8.3 Ma, and a new fault system developed. Northwest-trending dextral-slip faults formed to the northwest of the raisen batholith, whereas the northeast-trending South Damxung thrust faults with some sinistral-slip formed to the southeast. The latter are replaced farther to the east by the west-northwest-trending Lhünzhub thrust faults with dextral-slip. This relatively local uplift that left adjacent Eocene and Miocene deposits preserved was followed by a regional uplift and the initiation of a system of generally north-south grabens in the Late Miocene at ~6.5 Ma. The regional uplift of the southern Tibetan Plateau thus appears to have occurred between 8.3 Ma and 6.5 Ma. The Gulu, Damxung-Yangbajain and Angan graben systems that pass east of the Nyainqêntanglha Mountains are locally controlled by the earlier northeast-trending faults. These grabens dominate the subsequent tectonic movement and are still very active as northwest-trending dextral-slip faults northwest of the mountains. The Miocene is a time of great tectonic change that ushered in the modern tectonic regime.

Key words: Miocene tectonics, strike-slip fault, thrust fault, extensional tectonic system, uplift, granite plutonism, Nyainqêntanglha region, Tibetan Plateau

1 Introduction

The Miocene is an important time in the history of the Tibetan Plateau during which it reached its present elevation (Dewey et al., 1988; Harrison et al., 1992, 1995; Copeland et al., 1995; Blisniuk et al., 2001; Tapponnier et al., 2001; Spicer et al., 2003). However, Miocene tectonic movements were not well known due to the lack of geologic data, and this has lead to uncertainty about the uplift history of the plateau. Now much more detailed geological mapping, organized by the China Geological Survey on the southern Tibetan Plateau, provides a thousand-fold increase of data with which we can understand the geologic processes and tectonic evolution in the Nyainqêntanglha region.

The region is dominated by the 7,000 m-high granite-cored Nyainqêntanglha Mountains that rise above the Nam Co Lake basin to the northwest and the Damxung-Yangbajain valley to the southeast. This vast region was investigated by geologic traverses every 3–5 km along the cross-valleys. We, together with others (2003) mapped the Damxung area, covering 30°00′ N to 31°00′ N by 90°00′ E to 91°30′ E, in the central part, Cheng et al. (2003) mapped the Xainza area, covering 30°00′ N to 31°00′ N by 88°30′ E to 90°00′ E, in the northwestern part, and Hu et al. (2003) mapped the Xigazê area, covering 29°00′ N to 30°00′ N by 88°30′ E to 90°00′ E, in the southwestern part. Regional geologic data from the other areas came

* Corresponding author. E-mail: wuzhenhan@yahoo.com.cn.

from Zhang et al. (1994), Li et al., (1993) and Pan et al. (2004). The INDEPTH survey provides deep seismic reflection and MT data below the Damxung-Yangbajain graben east of the Nyainqêntanglha Mountains (Brown et al., 1996; Chen et al., 1996; Nelson et al., 1996). These data, together with further studies in the field at key locations and a variety of laboratory work to date tectonic events, lead to important discoveries concerning high-angle dextral-slip faulting, thrust faulting, granite generation and extensional faulting of the Nyainqêntanglha region during the Miocene (Fig. 1). The work also found the northeast-trending Nyainqêntanglha thrust fault inferred by Tapponnier et al. (1986) and new constraints for the tectonic evolution and uplift history of the southern Tibetan Plateau. The discovery of the huge Nyainqêntanglha granitic complex, 138 km long by 15–25 km wide, above the Northwest Nyainqêntanglha shear zone has revealed that the Nyainqêntanglha Mountains does not consist of a Precambrian metamorphic rock series, the Nyainqêntanglha Group (Tibeten Bureau of Geology and Mineral Resources, 1993), as previously thought. The syntectonic complex, which consists of fine-grained granite in the outer part of the mountains and coarse-grained granite in the central part and was neglected by Kapp et al. (2005), lies between the northwest and southwest Nyainqêntanglha shear zones and represents a new tectonic feature.

The purpose of the paper is to integrate the relative ages and characters of movement of the faults found with absolute dates of the movement to show a more complete picture of the Miocene and later tectonic development of the Nyainqêntanglha region.

2 Geologic Setting and Tectonic Framework

The Nyainqêntanglha region has a long geologic record extending from Precambrian metamorphic rocks, exposed northwest of the Lake Nam Co (Hu et al., 2004), to Quaternary deposits in the Damxung-Yangbajain, Gulu and Angan grabens and the Nam Co basin (Wu et al., 2004b). Tectonic evolution of the region in the Paleozoic, Mesozoic and Early Cenozoic is closely related to successive spreading and northward subduction of the Paleo-oceanic Tethys plate (Dewey et al., 1988; Wu et al., 2004a). Subduction of Meso-Tethys in the Jurassic-Early Cretaceous resulted in not only the Bangoin-Nujiang suture, but also southward thrusting of ophiolites and tectonic slices in the West Nam Co thrust at the western shore of the Nam Co Lake (Wu et al., 2004b). Later subduction of the Neo-Tethys resulted in the Yarlung Zangbo suture, east-west folds and thrust faults, Gangdise batholith and volcanic-sedimentary strata of the Linzizong Group. The subsequent continental plate collision of Indian with Asia, at ~50 Ma, caused crustal shortening of about 50% by thrusting and folding in the Tibetan Plateau. This gave rise to the Gangdise thrust system in the southern Lhasa block in the early Tertiary (Yin et al., 1994), the Main Central thrust and South Tibet detachment thrust faults in the Early Miocene (Harrison et al., 1992; Yin and Harrison, 2000), and the Main Boundary thrust in the Himalayan block in the Late Miocene (Zhao et al., 1993) (Fig. 1) along with widespread contractional structures in the Qiangtang block of the northern Tibetan Plateau in the Tertiary (Kidd et al., 1988). Lateral strike-slip faulting and eastward extrusion dominated in the Tibetan Plateau since the Late Oligocene (Tapponnier et al., 1986, 2001), along with east-west crustal extension after the Late Miocene (Harrison et al., 1995; Blisniuk et al., 2001).

The principal structure of the Nyainqêntanglha region consists of several fault systems of different characteristics. They cut Tertiary strata, such as the Paleocene-Eocene Linzizong and Miocene Wuyu groups and various Tertiary granites, including the Late Cretaceous-Early Tertiary Gangdise batholithic complex, a Paleocene-Eocene complex and an Oligocene pluton (Figs. 1 and 2). The Gangdise fault system and Gangdise shear zone, which are dominated by dextral-slip and southward oblique-thrust offset, lie southwest of the Nyainqêntanglha Mountains (Fig. 2a). They curve into the Nyainqêntanglha Mountains where the northeast-trending, southeast-dipping Nyainqêntanglha thrust system, comprised of the North, Northwest and Southwest branches, encompass the Miocene Nyainqêntanglha granitic batholith (Liu et al., 2004; Wu et al., 2004a). These, in turn, curve eastward into the dextral-slip, south-dipping North Damxung shear zone and Jiali fault zone. A relatively short Guren Qu shear zone cuts across the granite complex. Northwest of all of these faults are a series of northwest-trending dextral-slip faults of the Karakorum-Jiali system, and southeast of the Nyainqêntanglha Mountains lies the sinistral-slip South Damxung thrust system crossed by the younger Angan, Damxung-Yangbajain and Gulu grabens with their bounding normal faults (Figs. 1 and 2b). Farther east there lie the North Lhünzhub thrust faults and the East Yangbajain shear zone dominated by dextral-slip and southward oblique-thrust offset (Fig. 2b).

The major structural systems also served as boundaries of stratigraphic regions (Fig. 3), which indicate their tectonic significance in separating blocks with different volcanic-sedimentary histories. The North Nyainqêntanglha thrust separates the Lhasa stratigraphic region and the Xainza stratigraphic region in the west, and

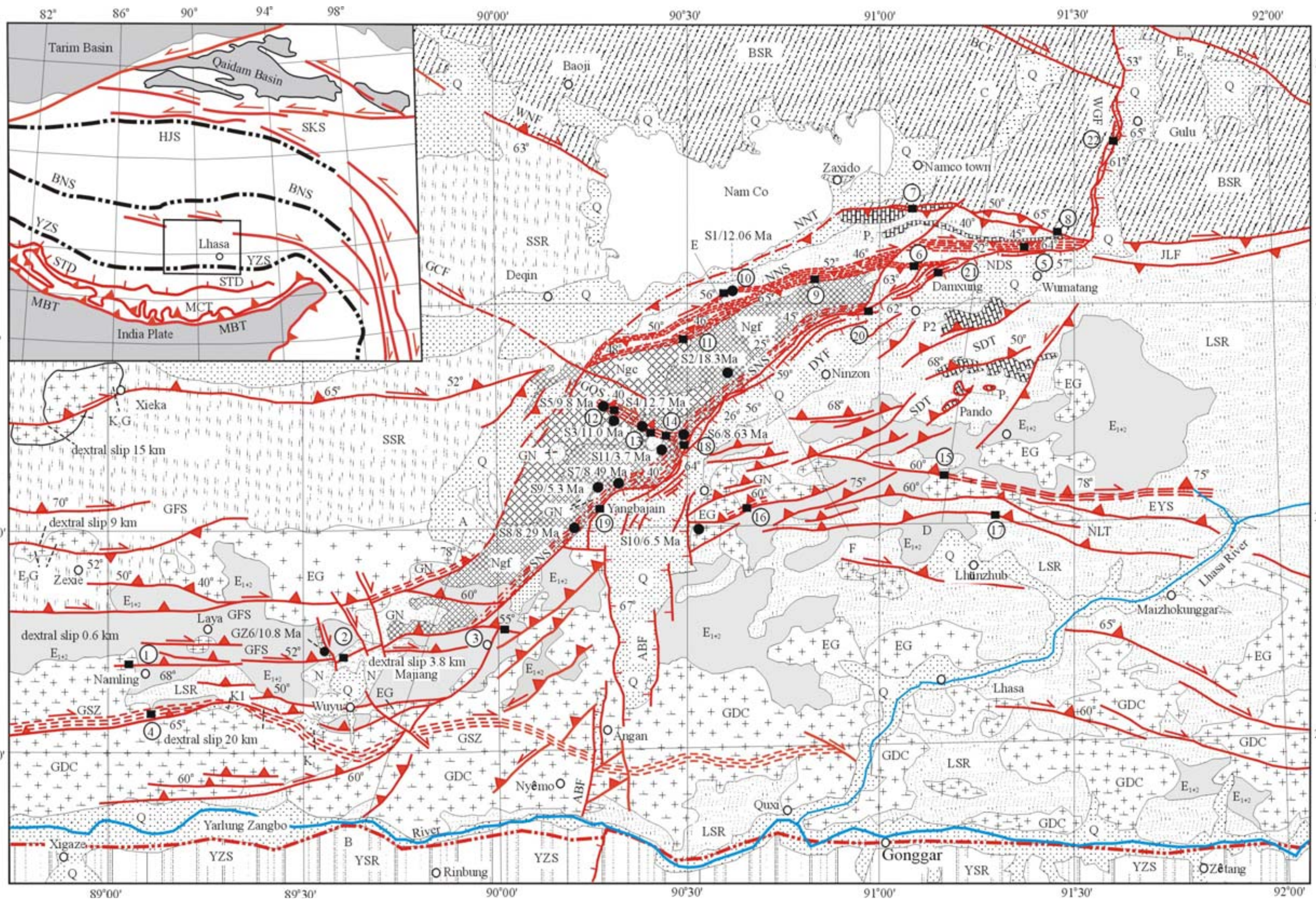

Fig. 1. Geologic map of the Nyainqêntanglha region, southern Tibetan Plateau.

Q – Quaternary deposits of gravel, sand and clay; N – Miocene volcanic–sedimentary strata of the Wuyu Group composed of conglomerate, sandstone, andesite, dacite, and trachite; E_{1+2} – Paleocene-Eocene volcanic-sedimentary rocks of the Linzizong Group dominated by andesite, rhyolite, dacite, trachite, basalt, sandstone and conglomerate; P_2 – Upper Permian limestone; LSR – Lhasa stratigraphic region; BSR – Bangoin stratigraphic region; SSR – Xainza stratigraphic region; YSR – Yarlung Zangbo stratigraphic region; Ngc – Nyainqêntanglha coarse-grained granite; Ngf – Nyainqêntanglha fine-grained granite; GN – gneiss; E_3G – Oligocene granite; EG – Eogene granitic rocks mainly formed in Paleocene-Eocene; GDC – Gangdise batholitic complex formed in Late Cretaceous to Eocene; K_2G – Late Cretaceous granite. NNT – north Nyainqêntanglha thrust fault; NNS – northwest Nyainqêntanglha shear zone; SNS – southeast Nyainqêntanglha shear zone; SDT – South Damxung thrust fault; NLT – North Lhünzhub thrust fault; GQS – Guren Qu shear zone; GSZ – Gangdise shear zone; NDS – North Damxung shear zone; EYS – East Yangbajain shear zone; GFS – Gangdise fault system; JLF – Jiali fault; DYF – Damxung-Yangbajain fault system; ABF – Angan boundary fault system; WGF – West Gulu fault system; BCF – Bengco strike-slip fault; GCF – Gerenco strike-slip fault; WNF – West Nam Co strike-slip fault; black circle: sampling location for dating with age marked in nearby; black square: field outcrop; A-B, C-D and E-F – position of the cross-section. The inset of the Tibetan Plateau on the upper left shows the location of the Nyainqêntanglha region by a square; SKS – South Kunlun suture; HJS – Hoh Xil-Jinsha suture; BNS – Bangoin-Nujiang suture; YZS – Yarlung Zangbo or Indus-Yarlung Zangbo suture.

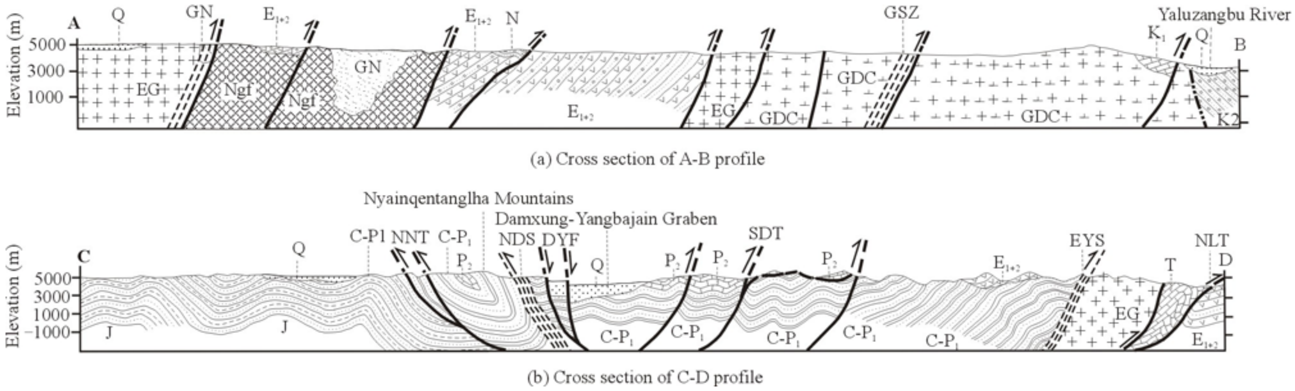

Fig. 2. Cross sections A-B and C-D across the Gangdise fault system and the Nyainqêntanglha Mountains respectively. The positions of A-B and C-D are shown in Fig. 1.

this fault in conjunction with the Jiali fault forms the boundary between the Lhasa and Bangoin stratigraphic regions in the east (Figs. 1 and 3). The major dextral-slip fault systems are considered to be dynamically related to thrust faults of the Nyainqêntanglha system, which, in turn, appear genetically related to the Nyainqêntanglha granite. The exposed granite seems linked down-dip with the partially melted crust indicated by the INDEPTH deep seismic reflection beneath the Damxung-Yangbajain graben to the southeast (Brown et al., 1996).

3 Major Fault Systems

3.1 The Gangdise fault system

The Gangdise fault system lies mainly north of the Gangdise granodioritic batholith southwest of the Nyainqêntanglha Mountains, but some faults cut this batholith and it was thus called the Gangdise thrust system by Harrison et al. (1992) and Yin et al. (1994). These east-west faults also offset Paleocene-Eocene strata and granites (Figs. 1 and 2a). Most faults in the system dip 50°–70° northward, and form fault zones hundreds of meters wide containing tectonic schist, mylonite, breccia, minor folds, lens slices and cleaved rocks. Some faults dip southward with high dip angles of 50° or more. The major faults show lateral dextral-slip in horizontal view (Fig. 1) and oblique-thrust offset in cross section (Fig. 2a), and have oblique slickensides (Fig. 4a). Lateral dextral-slip on a single fault may reach ~15 km, as shown by offset of Late Cretaceous granite west of Xieka. Lateral offsets of Oligocene granite north of Zexie and Eocene granite south of Laya are ~9 km and 0.6 km respectively. The fault branch between Namling and Majiang shows both a 3.8 km dextral-slip displacement of Oligocene-Miocene strata and southward thrust offset accompanied by overturn folds of Miocene strata in the northeastern Wuyu basin (Figs. 1, 2a and 4b). This fault displays dextral-slip slickensides north of Namling (Fig. 4a) and thrust motion by convergence cleavage in Eocene volcanic rocks of the Linzizong Group near site 3. The fault system gradually curves east-northeastward towards the Nyainqêntanglha Mountains, except for one broad shear zone that continues eastward along the southern part of the system (Fig. 1). Harrison et al. (1992) considered the latter separately from the thrust system, but the shear zone merges westward into high-angle faults of the Gangdise fault system southwest of the Nyainqêntanglha Mountains and has undergone similar movement, so it is grouped with them. The Gangdise shear zone exhibits ~20 km dextral-slip offset of the Gangdise batholith and Early Cretaceous volcanic-sedimentary strata south of the Wuyu basin (Fig. 1), and some oblique-thrust is indicated by folds in mylonitic schist and foliation in the south of Namling as granitic mylonite of GSZ at site 4.

3.2 The North Damxung shear zone-Jiali fault zone

The North Damxung shear zone extends east-west along the north side of the Damxung basin, northeast of the Nyainqêntanglha Mountains (Fig. 1). The shear zone extends more than 50 km west of the Quaternary normal faults of the Gulu graben. East of the graben it appears to have merged with the Jiali fault zone, which also exhibits a wide shear zone. Farther west the North Damxung shear zone appears to tie in with shearing in the Nyainqêntanglha thrust system, and it is dominated by dextral-slip shearing and characterized by a quartz-feldspar and quartz-mica mylonite zone, 2,000–2,500 m wide north of Wumatang. Two branches of tectonic schist are present north of Damxung; the southern branch 800–1,200 m wide and the northern one 2,000–3,000 m wide (Fig. 1). The foliation of the mylonite mainly dips 65°–80° southward near site 5. Quartz and feldspar within mylonite show a silk-like structure of thinly elongated quartz from ductile deformation and re-crystallization with some feldspar porphyroblasts scattered along the foliation (Fig. 4c). Microscopic structures of the mylonite show

Stratigraphic Region	Yarlung Zangbo (YSR)	Lhasa (LSR)	Xainza (SSR)	Bangoin (BSR)
Holocene (Q_4)	fluvial, alluvial and lacustrine deposits: sands, pebble and mud			
Pleistocene (Q_{1-3})	glacial, lacustrine, fluvial and alluvial deposits: pebble, sands, silt and clay			
Miocene (N)		Wuyu Group : andesite, dacite, shale, sandstone	Wuyu Group : andesite, dacite, shale, sandstone	Kangtuo Formation: sandstone, siltstone and mudstone
Oligocene (E_3)			sandstone, limestone	Dinqin Formation: sandstone, mudstone
Eocene (E_2)		Linzizong Group: dacite, andesite and sandstone	Linzizong Group: dacite andesite and sandstone	Niubao Formation: mudstone, sandstone
Paleocene (E_1)				
Upper Cretaceous (K_2)		Shexing Formation: sandstone, mudstone and conglomerate	Jingzushan Formation: conglomerate, shale and sandstone	Jinzushan Formation: conglomerate, sandstone
Lower Cretaceous (K_1)	Jiabula Formation: shale, sandstone and silicalite	Takena, Chumulong and Linbuzong Formations: sandstone and limestone	Lajiangshan Formation: sandstone, siltstone and conglomerate	Langshan Formation: limestone and shale; Doni Formation:shale, limestone
Upper Jurassic (J_3)	Weimei Formation: sandstone and shale	Duodigou Formation: limestone and shale	Wuolongou Formation: andesite and sandstone	Lagongtang Formation: sandstone, conglomerate
Middle Jurassic (J_2)	Zela Formation: shale and silicalite	Qiesanwenquan Group: shale and siltstone	Jienu Group: basalt, andesite and sandstone	Sankalayong Formation: sandstone, mudstone
Lower Jurassic (J_1)	Redang Formation: limestone and shale	Jialapu Formation: siltstone and sandstone		
Upper Triassic (T_3)	Nieru Formation: plate and meta-sandstone	Mailongang Formation: limestone, shale and siltstone		Quehala Group: meta-sandstone and silicalite, marble
Middle Triassic (T_2)		Chaqupu Formation: dacite, andesite and limestone		
Lower Triassic (T_1)				
Upper Permian (P_3)		Mongla Formation: limestone and shale	Jianzalong Formation: dolomite and limestone	
Middle Permian (P_2)		Luobadui Formation: limestone and silicalite	Xiala Formation: limestone	
Lower Permian (P_1)		Laigu Formation: sandstone and siltstone	Angjie Formation: sandstone, conglomerate	
Upper Carboniferous	?	Nuoco Formation:plate, metasandstone, siltstone and conglomerate	sandstone, limestone	
Lower Carboniferous			Yonzhu Formation: sandstone and siltstone	?
Devonian (D)			Chageloma and Dardong Formations: limestone	
Silurian (S)			Meta-sandstone and silicalite	
Ordovician (O)			Ganmusang and Kerdo Formations: limestone	
Cambrian (Є)				
Proterozoic (Pt)	Laguigangri Complex: mica schist and gneiss	Metamorphic complex: gneiss, amphibolite and schist	Metamorphic complex: gneiss, amphibolite and schist	

Fig. 3. Stratigraphic columns for the various stratigraphic regions in the Nyainqêntanglha region.

recrystallization of quartz and clockwise rotation of feldspar porphyroblasts, indicating dextral shearing of mylonite and dextral-slip.

The tectonic schist contains some pebbles of Carboniferous conglomerate, which are stretched 4–6 times longer than their original shape after dextral-slip and shearing along with the east-west foliation, pen-structures and dense cleavage (Fig. 4d). Lineation and slickensides strike east-west with plunges less than 10° at site 6 north of Damxung. The southern zone cuts Eocene volcanic rocks of the Linzizong Group, forming mylonitic andesite and showing metamorphic effects of green-schist facies. New minerals formed during metamorphism include chlorite, chloritoid, mica, garnet and staurolite along with hornblende, which is found only in the northern zone.

3.3 The Guren Qu shear zone

The Guren Qu shear zone trends northwest across the Nyainqêntanglha granite along the Guren Qu valley north of Yangbajain, and has a general width of 300–600 m, but may reach 1,000–1,500 m at some localities. The shear zone dips northeast at 35°–45° and extends ~20 km, from

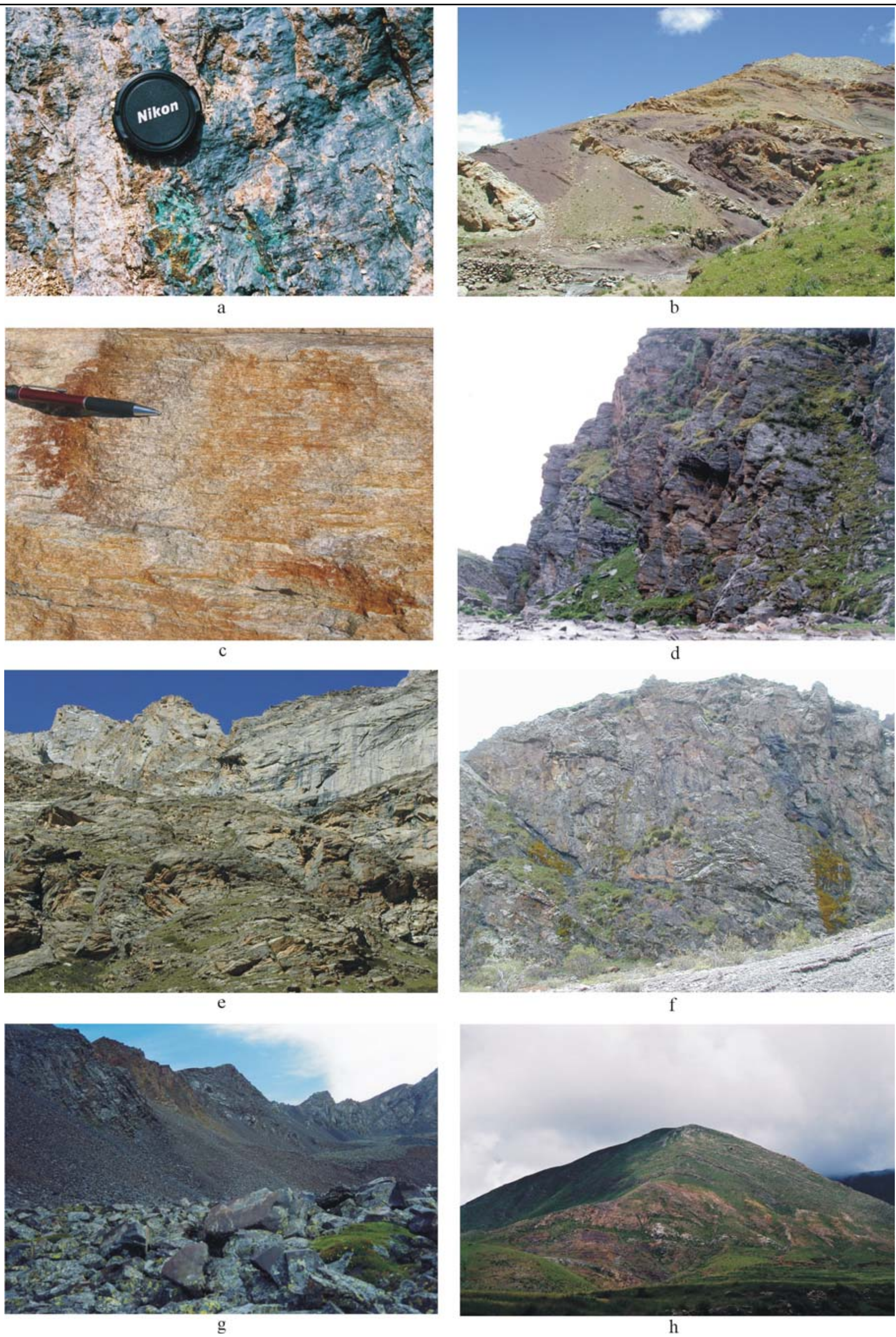

Fig. 4. Photographs of typical fault systems of the Nyainqêntanglha region and its vicinities.

a – a view northwest at slickensides indicating dextral-slip of the Gangdise fault system, GFS, at site 1; b – a view northward at folds in sandstone and shale of the Wuyu Group formed by dextral-slip and oblique thrust of fault at site 2; c – a close-up view westward at mylonite of the north Damxung shear zone, NDS; d – a view southward at schist and lineation related to dextral slip of NDS at site 6; e – a view northeastward at granite overlying gneiss along the Guren Qu shear zone, GQS, at site 13; f – a view eastward at slightly metamorphosed Carboniferous sandstone thrust over Jurassic sandstone and shale along the north Nyainqêntanglha thrust fault, NNT; g – a view southward at Upper Permian limestone thrust over Jurassic sandstone along the North Nyainqêntanglha thrust fault, NNT, west of site 8; h – a view northward at Triassic limestone thrust over Late Cretaceous reddish sandstone and shale along North Lhünzhub thrust fault, NLT, at site 17.

where it is cut off by the Southeast Nyainqêntanglha shear zone and Damxung-Yangbajain normal faults (Fig. 1). The zone's mylonitic foliation, which locally imparts a thinly-layered like appearance to the granite near site 12, makes a clear boundary with the weakly deformed Nyainqêntanglha granite. The sheared rocks consist of granitic mylonite, mylonitic granite and quartz-mica schist with lens structures forming S-C textures that indicate dextral shearing. The low dip suggests a thrust component as well. Quartz and feldspar lenses contain porphyroblasts surrounded by recrystallized fine quartz and mica, which form foliation and mica-fish structure as granitic mylonite from site 14. The Guren Qu shear zone offsets both the granite and enclosed gneiss that may be tightly folded. The dextral-slip shearing results in the granite overlying the gneiss in the eastern part of the zone (Fig. 4e).

3.4 The East Yangbajain shear zone

The East Yangbajain shear zone is an important structure and extends more than 100 km eastward from the Damxung-Yangbajain graben. It exhibits dextral-slip offset of a Paleogene granitic batholith and Paleocene-Eocene volcanic-sedimentary strata of the Linzizong Group (Fig. 1). The western part is a mylonitic ductile shear zone, which gradually changes eastward into a more brittle zone. The western section of the fault zone appears as a ductile shear zone 400–1,200 m wide occupied by mylonitic granite, granodiorite and andesite and also quartz-mica and quartz-feldspar mylonite. The zone contains lens structures, minor folds, S-C texture and lineation. The lens structure is formed of feldspar and quartz-feldspar porphyroblasts, 0.2–0.6 mm wide and 1.0–2.5 cm long, and surrounded by mica and elongated quartz foliation. Pressure shadows of rotated porphyroblasts sampled at site 15 indicate dextral-slip and the lineations plunge less than 15° in an east-west alignment. Carboniferous conglomerate and sandstone and Permian limestone are thrust over Eocene volcanic-sedimentary strata of the Linzizong Group and Paleogene granite along the high-angle, north-dipping fault (Fig. 2b).

The eastern section dips 50°–70° northward and displays breccia, cleavage, lens structure and oblique lineation of sericite and chlorite in slickensides, which all indicate major dextral-slip. Carboniferous conglomerate and sandstone of low metamorphic grade are obliquely thrust southward over Eocene volcanic rocks and accompanied by minor folds, whose axial planes dip southward in the hanging wall.

3.5 The Karakorum-Jiali strike-slip fault system

A series of widely spaced en echelon northwest-trending dextral-slip faults, found northwest of the Nyainqêntanglha Mountains, form components of the Karakorum-Jiali strike-slip fault system of the southern Tibetan Plateau (Armijo et al., 1989; Geology Institute of CSB, 1992). These include the Bengco, Gurenco, West Nam Co and other faults (Fig. 1).

The Bengco fault is 100–120 km long and made up of 3 major segments (Geology Institute of CSB, 1992; Wu et al., 2005). Offset bedrocks, ridges, streams, glacial valleys and lake terraces show a dextral-slip rate along the fault of 7–16 mm/a in the Late Pleistocene-Holocene. The fault forms an important regional seismic zone and is the site of the magnitude M_s-8.0 Bengco earthquake of 1951 and several strong earthquakes during the Holocene. Seismic fractures, pressure ridges, sag ponds and pull-apart basins formed along ~81 km of the fault during the earthquake and ~8 m of dextral-slip occurred near its epicenter. The average strike-slip rate and interval of M_s -8.0 earthquakes in the Late Pleistocene-Holocene are estimated at 11.5±4.5 mm/a and 900±500 a, respectively, for the Bengco fault (Wu et al., 2005).

The Gerenco fault, another major component of the Karakorum-Jiali strike-slip fault system, extends up to ~230 km from the west of the Gerenco Lake to the south of Deqin. It also displays dextral-offset of bedrocks, ridges and streams and forms seismic fractures and the northwest-trending Gerenco pull-apart basin. Two intense earthquakes, M_s-6.5 in 1934 and M_s-6.6 on February 22, 1980, occurred along the fault with the epicenters located west and east of the Gerenco Lake, respectively. Dextral displacement along the Gerenco fault was as large as 500 m in the late Quaternary, and the dextral-slip rate of the middle segment of the fault is estimated to be 2.0–4 mm/a in the Late Holocene according to the Geology Institute of CSB (1992).

The 25 km long West Nam Co fault lies northwest of the Nam Co Lake, where it offsets ridges, Permian limestone and Upper Cretaceous sandstone in a right-lateral fashion and forms breccia 20–50 m wide. Its exposed middle section is seen to dip 80°–85° northeastward, but its northwest and southeast sections are covered by Middle Pleistocene-Holocene fluvial, alluvial and lacustrine deposits. The West Nam Co fault offsets earlier thrust faults of the North Nyainqêntanglha thrust (Wu et al., 2004a), controls the linear distribution of hot springs and epicenters of earthquakes with magnitudes of 4.0 to 5.6 northwest of the Nam Co Lake, and appears to extend southeastward across the Nam Co Lake. However, the slip-rate of the West Nam Co fault is smaller than 1.5 mm/a since the Late Pleistocene (Wu et al., 2003) and it appears to be a minor component of the Karakorum-Jiali strike-slip fault system.

3.6 The Nyainqêntanglha thrust system

The Nyainqêntanglha thrust system consists of three major northeast-trending, southeast-dipping thrust faults that encompass the granite-cored Nyainqêntanglha Mountains. The Northwest and Southwest Nyainqêntanglha shear zones border those sides of the Nyainqêntanglha granite, and the North Nyainqêntanglha fault lies a little north of the granite (Fig. 1). The North thrust appears to be of the same age as the Northwest shear zone and merges with it to the northeast. A thrust on the northwest side of the mountains was predicted by Tapponnier et al. (1986), but was not supported by field data until now. These thrusts seem to join with the faults of the Gangdise system to the southwest, but the connection is obscured by a Pleistocene cover. The Gangdise faults steepen to 80° to the north as they approach the thrusts and look as if they are rolling over into the southeast-dipping thrust faults. The thrusts also converge northeastwards towards the North Damxung-Jiali faults.

The North Nyainqêntanglha thrust fault zone consists of oblique-thrust faults exposed north of the mountains, but its southwestern section is buried beneath thick Quaternary glacial and lacustrine deposits southeast of the Nam Co Lake. The major exposed faults in the zone dip 45°–60° southward, but a few minor ones dip northward. Upper Permian limestone is thrust northward over Lower Cretaceous reddish conglomerate and sandstone south of the town of Nam Co and metamorphosed Carboniferous conglomerate and sandstone are thrust northward over Jurassic sandstone north of Wumatang (Fig. 4f). The bedding in the Upper Permian limestone is obscured by dense cleavage near a major fault south of the Zaxido Peninsula and overturned south-dipping anticline and syncline formed in Carboniferous-Permian strata of the hanging wall (Fig. 2b). The fault is separated into two main branches in the west of site 8; Upper Permian limestone is thrust northward over Jurassic sandstone along the larger northern branch and the smaller southern fault lies within the Upper Permian limestone (Fig. 4g).

The Northwest Nyainqêntanglha shear zone is exposed near the northwest border of the Nyainqêntanglha granite and generally dips 46°–56° southeastward in the southeast of site 10, but reaches 65° at some localities (Fig. 1). The shear zone is about 75 km long and the width ranges between ~200 m to 3.2 km. The major part of the shear zone is along the northwest margin of the granite, which has been thrust northwestward over metamorphosed Carboniferous sandstone and conglomerate, although some branches lie within the Carboniferous strata in the western part.

The Northwest Nyainqêntanglha shear zone appears as a wide zone of mylonitic granite, granitic mylonite, quartz-feldspar mylonite and quartz-mica schist, and has a variety of shear structures such as feldspar lens structure, S-C texture, foliation of mica and lineation of elongated quartz and cleavage (Fig. 5). Here, the foliation and cleavage make the granite appear laminated (Fig. 5a). The mylonite foliation consists of biotite, muscovite, sericite and elongated quartz. Quartz grains of the granite have been recrystallized during ductile shearing (Fig. 5c) and many feldspar grains appear as rotated porphyroblasts that indicate dextral shearing and thrusting of the hanging wall (Fig. 5b). Where the outer fault branch lies within metamorphosed Carboniferous-Lower Permian sandstone and conglomerate, pebbles are elongated 3–6 times their original lengths and the thick beds of strata are replaced by thin slices of quartz-mica schist or quartz-sericite schist formed during ductile shearing (Fig. 5d). The mylonite schist, viewed under the microscope, is seen to consist of elongated and recrystallized sericite and quartz and the weakly deformed quartz appears as tiny porphyroblasts surrounded by foliation (Fig. 5e). Shearing in the coarse-grained granite resulted in mylonitic granite (Fig. 5f), granitic mylonite, quartz-mica mylonite (Fig. 5g) and quartz mylonite (Fig. 5h). Porphyritic feldspar crystals within the mylonite foliation are rotated (Fig. 5f). The biotite grains and recrystallization of elongated quartz grains, seen under the microscope, also indicate dextral shearing and northwestward movement of the hanging wall (Fig. 5g and 5h).

Both fine- and coarse-grained Nyainqêntanglha granites are thrust northwestward over the Carboniferous Nuoco Formation and Lower Permian Laigu Formation along with some lateral-slip. Dextral offset of quartz veins as well as oblique lineations are seen in places (Fig. 1). Northward dipping foliations occur locally within the granite and several granite and diorite veins along with northward dipping faults, 5–8 km long and hundreds of meters wide, are present in the Upper Carboniferous-Lower Permian strata northwest of the granite (Fig. 1). In addition, many northeast-trending folds in adjacent strata (Wu et al., 2003) may be due to the thrust movement.

The Southeast Nyainqêntanglha shear zone was called the Nyainqêntanglha shear zone by Pan and Kidd (1992) and Harrison et al. (1995), but has been renamed following the discovery of the Northwest Nyainqêntanglha shear zone. The Southeast shear zone extends northeastward more than 100 km and is 1–3 km wide. The major part of the shear zone bounds the southeastern margin of the Nyainqêntanglha granite, but a small portion passes through metamorphosed Carboniferous sandstone and conglomerate. This southeastern ductile shear zone consists of granitic, quartz-mica and quartz-feldspar

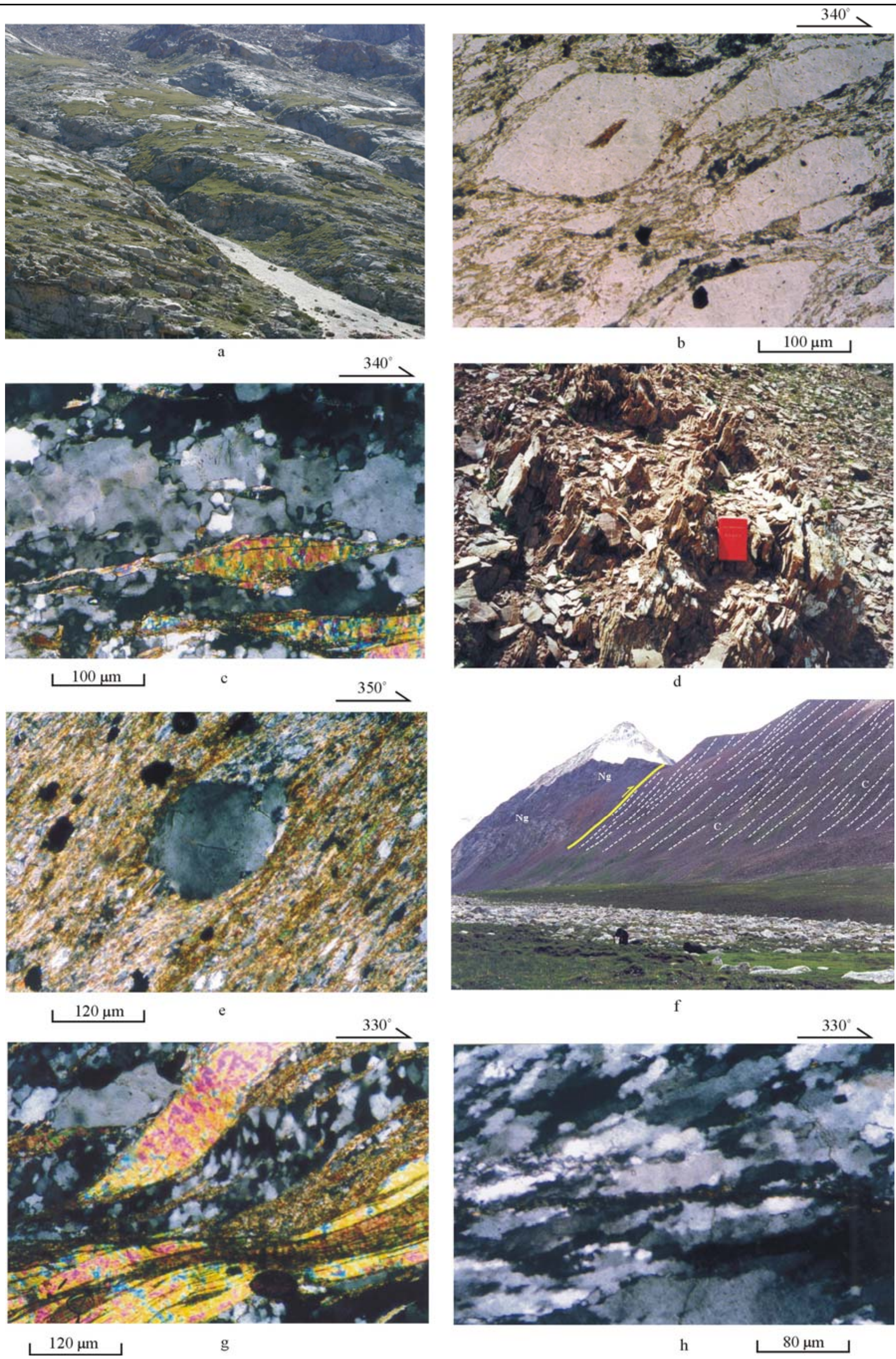

Fig. 5. Photos of granitic mylonite of the Northwest Nyainqêntanglha shear zone, NNS, east of the Nam Co Lake.

a – a view southward at site 9; b – a microscopic view of lens structure indicating dextral rotation of feldspar at site 9; c – a microscopic view of schist foliation at site 9; d – a view westward at mica quartz schist foliation at site 10; e – a microscopic view of shear foliation of mica quartz schist at site 10; f – a view southward at Nyainqêntanglha granite thrust over Carboniferous sandstone and conglomerate along the Northwest Nyainqêntanglha shear zone, NNS, southeast of site 10; g – a microscopic view at foliation from site 11 indicating dextral shearing; h – a microscopic view of shear foliation and recrystallized quartz from site 11.

mylonites with foliation dipping gently southeastward; ~25º in the mid-fault and 10º–20º less than the Northwest zone (Fig. 6a), but most of the zone dips steeply. The lens structure (Fig. 6b) and S-C texture indicate that the upper plate has moved relatively southeastward. The elongation of the quartz, seen under the microscope, is formed during recrystallization under ductile shearing, which also generated mica (Fig. 6c) and lenses with rotated feldspar porphyroblasts (Fig. 6d). The thickness of porphyroblasts and lenses generally ranges from less than 100 microns (Fig. 6d) to several millimeters, and some reach more than 10–15 mm in the margin of the zone. Plastic flow in enclosed gneiss and in the metamorphosed Carboniferous strata above the fault caused flow structures, lens structures, feldspar-quartz elongation and new metamorphism to green-schist facies within and near the shear zone. Some of these minor structures also indicate the down-dip movement.

The Southeast Nyainqêntanglha shear zone has similar features as the Northwest one, which was also formed at depths where pressure and temperature promoted recrystallization and mild metamorphism. Pan and Kidd (1992) referred to it as an extensional shear zone, based on small-scale features seen at three locations, and Harrison et al. (1995) considered the possibility that it originally had the steeper dip of a normal fault, but had been rotated to a gentle dip. The shear zone does not display the shallow extensional features of a normal fault, and a rotation of the fault, which is already steep in most places, would give it a northwest dip locally. Mapping shows it to be a thrust fault and not an extensional detachment fault as proposed. Also, no other extensional shear has been found in the region. The down-dip features may be due to some gravitational back-sliding, similar to that along the South Tibet Detachment (Yin and Harrison, 2000) (Fig. 1), perhaps as the granite rose later. Such back-sliding features are common along the deep thrust faults of southern New England. Both border shear zones apparently originated as local concentrations of the movement that produced the flow-foliation in the granite and dated from the time of its origin. Continued movement as the granite cooled produced the shearing. The under-thrusting is clearly seen on the northwest by offset and shown for both faults in the regional structural pattern. Thrusting also affected the granite in places along the nearly contemporaneous Guren Qu shear zone.

3.7 The South Damxung thrust fault system

The South Damxung thrust fault system mainly consists of a broad band of northeast-trending faults with northwestward dips of 50° to 75°, which lie southeast of the Nyainqêntanglha Mountains. Permian limestone and Carboniferous sandstone and conglomerate of low metamorphic grade are thrust over Upper Cretaceous reddish conglomerate and Eocene volcanic rock and granite. Nappes of Upper Permian limestone over Carboniferous strata occur at some localities (Fig. 1). Some northeast-trending folds, 10–15 km long, are present in the hanging wall (Fig. 2b), and minor drag-folds, breccia, lens structures, schist, cleavage and slickensides indicating oblique-thrust are seen in the major fault zones. Portions of faults contain veins of granite, granodiorite, quartz and calcite of a dozen centimeters to several meters in width and hundreds of meters to several kilometers long. The faults west of the Angan graben and some southeast of the Damxung-Yangbajain graben exhibit sinistral-slip offset of Eocene volcanic rocks and granite, besides oblique-thrust offset, and cause lateral dislocation of earlier, mainly east-west-trending folds and thrust faults (Wu et al., 2004a).

One South Damxung thrust fault forms a ductile shear zone 120–250 m wide with lenses and silk-like structures, S-C textures and mylonite schist southeast of Yangbajain (Fig. 1). The original bedding of the Carboniferous-Lower Permian strata is completely replaced by mylonite foliation with dips of 60°–70° as site 16. Pebbles of Carboniferous conglomerate are elongated several times their original lengths and form vein-like quartz-feldspar structures along the foliation.

3.8 The North Lhünzhub thrust fault system

The North Lhünzhub thrust fault system lies south of the East Yangbajain shear zone (Fig. 1). The major faults extend west-northwest with low northward dips of ~30°–45°, and are often accompanied by northward overturned folds in the hanging walls (Fig. 2b). Triassic limestone and metamorphosed Carboniferous sandstone and conglomerate are thrust relatively southward over Upper Cretaceous reddish sandstone and shale (Fig. 4h) and Eocene volcanic rocks and limestone to form nappes north of Lhünzhub. Breccia 30–250 m thick, cleavage, overturned minor folds, slickensides, lenses and pudding structures in fault zones near site 17 indicate thrusting. Two fault breaks occur along the fault zone at some localities. The western ends of some faults curve west-southwest and appear to merge with faults of the South Damxung system, which suggest that they are contemporaneous.

3.9 Graben boundary fault systems

Normal faults occur as boundary systems for the line of grabens that cross the region east of the Nyainqêntanglha Mountains and are referred to by the name of their respective graben: Gulu, Damxung-Yangbajain and Angan

(Fig. 1). They are part of a regional north-trending system that here trends northeastward in part, due to local control by the Southeast Nyainqentanghla shear zone. The faults, which are mostly along the west and northwest sides of the grabens, cut the shear zones and thrust faults, and remain very active (Fig. 6a). The West Gulu, Damxung-Yangbajain and Angan boundary fault systems are active mainly along the boundary between the grabens and the Nyainqêntanglha Mountains. Most faults are normal faults and dip between 56° and 70° southeastward or eastward, but several normal faults with opposite dips occur along the eastern boundaries (Fig. 1). Triangular facets, fault scarps (Fig. 6e), hanging valleys and offset Pleistocene glacial gravel and sand deposits occur along boundary faults and breccia is present in fault zones. Some well-lithofied breccia marks an early movement. Oblique lineation and slickensides (Fig. 6g), pressure ridges, en echelon and pull-apart basins along boundary faults (Fig. 6f) indicate lateral sinistral-slip in addition to vertical offset. Paleo-seismic fractures filled with Late Pleistocene-Quaternary sand and gravel are observed in trenches across the boundary normal faults that offset terraces of Late Pleistocene glacial deposits at site 21. Fractures and scarps of the Yangbajain earthquake of magnitude 8.0, which occurred in 1411 (Fig. 6e), and the North Damxung earthquake of M_s-7.5 in 1952 (Fig. 6h), formed along the major faults of Damxung-Yangbajain and West Gulu faults, respectively.

Slip-rates along the Damxung-Yangbajain and West Gulu faults are estimated from the displacement and age of Quaternary deposits cut by the normal faults. Vertical-slip rate of the Damxung-Yangbajain boundary faults is 0.5–1.0 mm/a during the Pleistocene and 0.4–2.0 mm/a in the Holocene with an average slip-rate of the Damxung-Yangbajain being 1.2 mm/a since the Late Pleistocene (Fig. 7a). The vertical slip-rate along the West Gulu changes from 0.4 mm/a to 1.2 mm/a in the Late Pleistocene and is 1.0–3.0 mm/a in the Holocene with an average of 2.0±1.0 mm/a (Fig. 7b). Sinistral-slip offsets of stream along the major faults of Damxung-Yangbajain and West Gulu faults are less than the vertical displacement, and the average sinistral-slip rates of these faults since the Late Pleistocene are less than 1.2 mm/a and 2 mm/a respectively.

4 Dating Tectonic Events

4.1 U-Pb isotopic dating of Nyainqêntanglha granite

Zircon grains from both fine- and coarse-grained varieties of the Nyainqêntanglha granite were selected for U-Pb isotopic dating by ion micro-probe on SHRIMP-II. All zircon grains used for U-Pb dating are euhedral and zoned from magmatic crystallization. The laboratory procedure and U-Pb isotopic data were described in detail by Liu et al. (2004). The $^{206}Pb/^{238}U$ ages of zircons from sample S3 (Fig. 1) range from 9.79 Ma to 12.22 Ma and yield a mean age of 11.0±0.2 Ma; the $^{206}Pb/^{238}U$ ages of zircons from sample S2 range from 17.07 Ma to 19.61 Ma and yield a mean age of 18.3±0.4 Ma (Liu et al., 2004). Mean ages of S3 and S2, 11.0±0.2 Ma and 18.3±0.4 Ma, respectively, well represent the granite age and provide time constraints for the shear zones along the borders and within the granite. Similar granite in the deep thrusts of the Northern Appalachian collision zone was generated in pulses (Barosh, 1991), perhaps in times of more active movement, and the age spread here may represent two such pulses. Sphene from a leucocratic vein, cutting a block of country-rock caught up in the Southeast Nyainqêntanglha shear zone, yielded ages of ~11 Ma (Copeland et al., unpublished, in Pan and Kidd, 1992). This may represent an offshoot of the younger pulse.

4.2 K-Ar isotopic dating of mylonite

Muscovite, biotite and K-feldspar selected from mylonite of the Northwest Nyainqêntanglha, Guren Qu and Southeast Nyainqêntanglha shear zones were used for K-Ar isotopic dating; the location of each sample is marked on Fig. 1. Sample S1 is quartz-mica schist from mylonite of the Northwest Nyainqêntanglha shear zone, S4 and S5 are granitic mylonite of the Guren Qu shear, and S6, S7 and S8 are quartz-feldspar schist from the Southeast Nyainqêntanglha shear zone mylonite. Dating of all these samples was done in the K-Ar Isotopic Laboratory of PetroChina in Beijing by using a MM 5400 vacuum isotopic spectrometer according to standard procedures. The isotopic ages are listed in Table 1.

The K-Ar isotopic age of S1 indicates that thrusting and shearing along the northwest side of Nyainqêntanglha granite developed until ~12 Ma, the Guren Qu dextral-slip shearing occurred at least during the period of 12.7–9.8 Ma after emplacement of the granite and the shearing along the southeast side of the granite continued into the Late Miocene with peak ages of 8.3–8.6 Ma (Table 1). These dates match well the previous $^{40}Ar/^{39}Ar$ thermal-chronological data on K-feldspar by Harrison et al. (1995). These isotopic ages also fit geologic relations between the Northwest and Southeast Nyainqêntanglha and Guren Qu shear zones and the age of the Nyainqêntanglha granite based on field relations (Fig. 1), even though there exist errors in the K-Ar isotopic dating. The ages thus provide reliable constraints for the times of tectonic movement in the Nyainqêntanglha region.

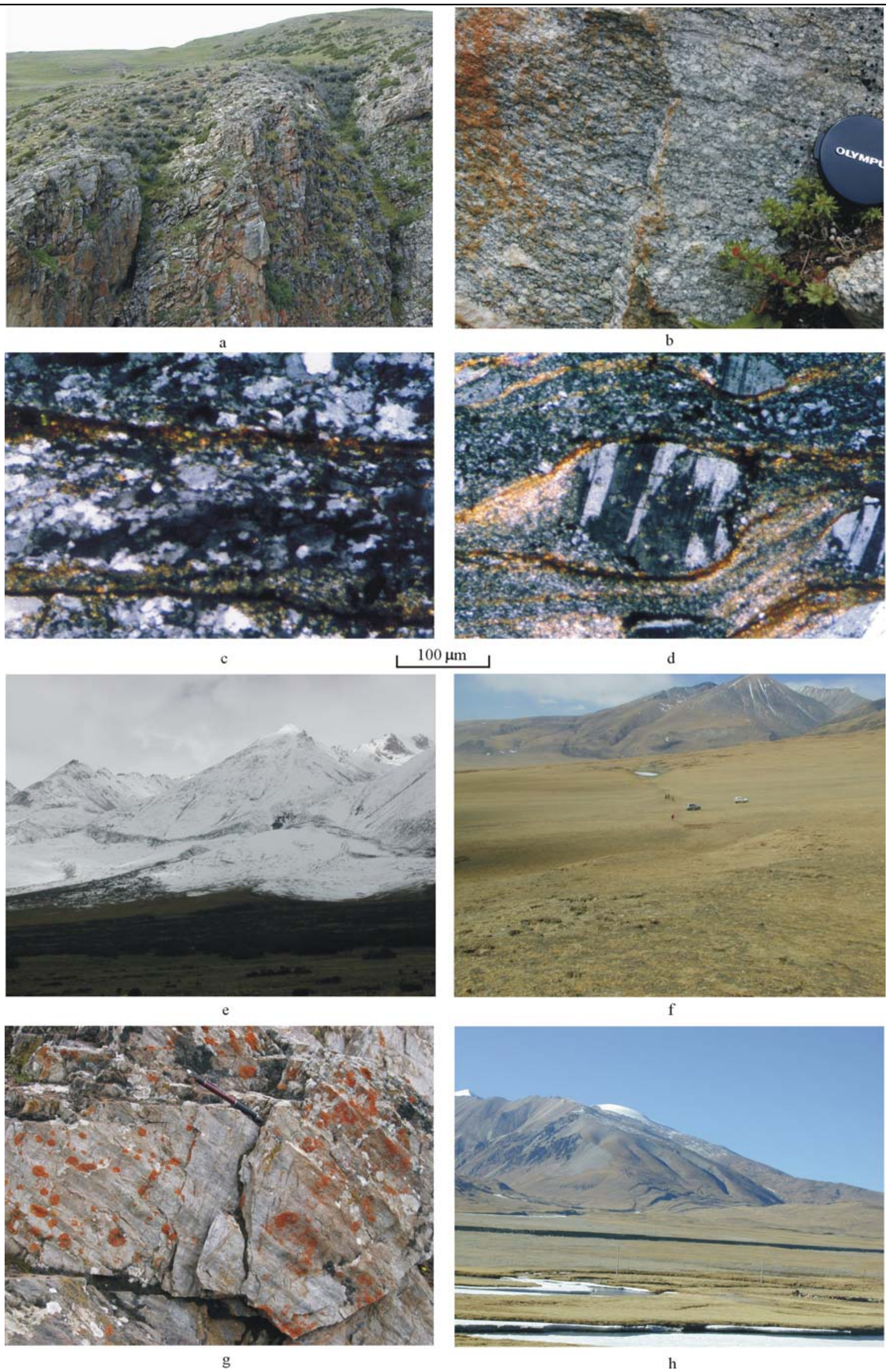

Fig. 6. Photos of the Southeast Nyainqêntanglha shear zone, SNS, and normal faults southeast of the Nyainqêntanglha Mountains.
a – a view southwestward at a high-angle normal fault cutting gently dipping mylonite schist at site 18; b – a close-up view northwestward at lens structure of granitic mylonite and schist at site 18; c – a microscopic view at granitic mylonite and schist at site 18; d – a microscopic view of feldspar lens structure indicating rotation and shearing at site 18; e – a view northwestward at normal fault scarp at site 19; f – a view westward at pressure ridge and pull-apart pond due to sinistral-slip at site 20; g – a close-up view at slickensides showing oblique-slip of the major boundary fault of the Damxung basin at site 20; h – a view northwestward at fractures from the 1952 M_s-7.5 earthquake along the West Gulu fault at site 22.

Table 1 K-Ar isotope data for dating of mylonite from the Nyainqêntanglha shear zones

Sample	S1	S4	S5	S6	S7	S8
Structure	NNS	GQS	GQS	SNS	SNS	SNS
Mineral	Muscovite	Biotite	Biotite	K-feldspar	Biotite	Biotite
K (%)	4.130	7.270	7.319	11.560	7.290	7.600
$^{40}Ar_{rad}$ (mol/g)	8.666E-11	1.609E-10	1.270E-10	1.734E-10	1.076E-10	1.095E-10
^{40}K (mol/g)	1.233E-7	2.170E-7	2.184E-7	3.450E-7	2.176E-7	2.268E-7
$^{40}Ar_{rad}/^{40}Ar_{total}$ (%)	35.94	64.86	44.16	64.68	46.54	38.67
$^{40}Ar_{rad}/^{40}K$	0.0007030	0.0007413	0.0005815	0.0005027	0.0004943	0.0004828
Age (Ma)	12.06±0.33	12.71±0.19	9.80±0.35	8.63±0.17	8.49±0.14	8.29±0.21

Note: Data $\lambda=5.543\times10^{-10}$/a, $\lambda_e=0.581\times10^{-10}$/a, $\lambda_\beta=4.962\times10^{-10}$/a and $^{40}K/K=1.167\times10^{-4}$ were adopted in age calculation. Explanation for the shear zones: NNS – Northwest Nyainqêntanglha; GQS – Guren Qu; SNS – Southeast Nyainqêntanglha.

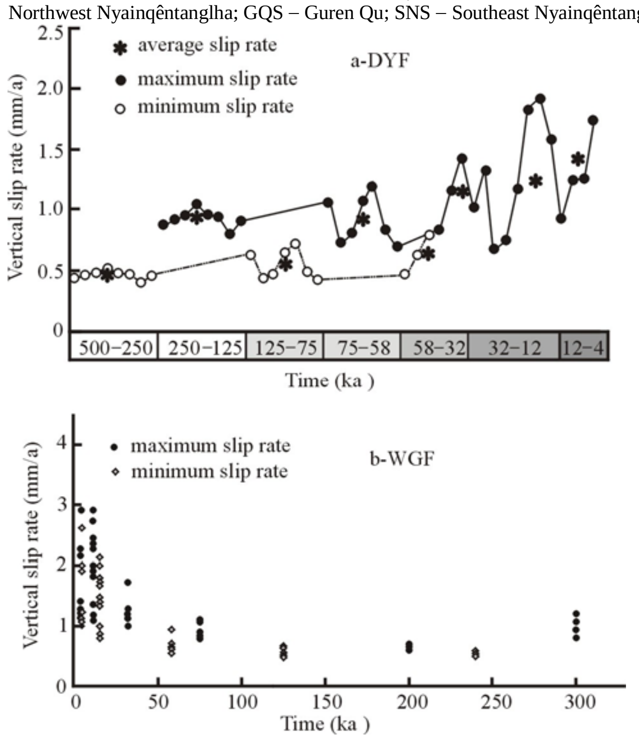

Fig. 7. Changes of the vertical slip rate of the Damxung-Yangbajain (a) and West Gulu (b) faults during the Quaternary. Maximum slip rate is calculated by the vertical displacement/minimum age of offset deposits and minimum slip rate is calculated by the vertical displacement/maximum age of offset deposits. Data for (a) taken from Wu et al. (2004).

4.3 Fission track dating of apatite from the Yangbajain and Nyainqêntanglha granites

Fission track dating was done for apatite selected from sample S10 of Eocene granite east of the Yangbajain basin and samples S9 and S11 of the Nyainqêntanglha granite northwest of the basin (Fig. 1). These samples were collected from outcrops of lower elevation at the boundaries of the Yangbajain basin and these ages should reflect the accelerated cooling due to normal faulting of the adjacent graben.

The fission track dating was accomplished by using the external detector method (Gleadow, 1981), along with calculations by zeta calibration (Hurford et al., 1982) using the Durango apatite, 31.4 Ma, as the age-calibration standard. The National Bureau of Standard trace element glass $SRM6_{12}$ was used as a dosimeter to measure the neutron fluencies during irradiation. Spontaneous fission tracks in apatite were etched in 7% HNO_3 at 20°C for 40 s. Induced fission tracks in the low-U muscovite external detectors that covered apatite grain mounts and glass dosimeters during the irradiation were later etched in 40% HF at 20°C for 20 minutes. Fission tracks and track length measurements were counted on an Olympus microscope by using a magnification of 1000 under oil immersion objectives for apatite. All analyses were performed in the Fission Track Laboratory of the Institute of Geology, China Seismological Bureau.

Fission track lengths of apatite exhibit a statistical pattern of a single peak for each sample and the central ages are 3.7±1.3 Ma, 5.3±0.5 Ma and 6.5±0.9 Ma, respectively, for S11, S9 and S10 (Fig. 8a, b and c). These fission track ages are lower than the K-Ar isotopic ages of the Southeast Nyainqêntanglha shear zone and should represent a rapid cooling in response to normal faulting of the Damxung-Yangbajain zone, which offsets the mylonite of the shear zone (Fig. 1). Assuming a closure temperature for fission track chronology of 100°C–120°C (Wagner and Van den haute, 1992; Wagner, 1998) and a geotherm of 35°C/km, which is 5°C/km higher than the continental average, the average vertical uplift rate of the Nyainqêntanglha Mountains is 0.77–0.93 mm/a and 0.54–0.65 mm/a at sampling locations S11 and S9, respectively, in the Quaternary, and the average vertical uplift rate of the Eocene granite at sampling location S10 is 0.44–0.53 mm/a since 6.5 Ma. The average uplift rate of the Nyainqêntanglha Mountains, 0.54–0.93 mm/a in the Quaternary is almost equal to the vertical-slip rate of the major Damxung-Yangbajain faults, 0.5–1.0 mm/a in the Pleistocene (Fig. 7a), which indicates that the uplift of the Nyainqêntanglha Mountains is closely related to the normal faulting in the Quaternary. It is further inferred that the initial time of extensional faulting of the Damxung-Yangbajain graben is 5.5–6.5 Ma, ~2–3 Ma later than the peak ages of ductile shearing along the Southeast Nyainqêntanglha shear zone (Table 1).

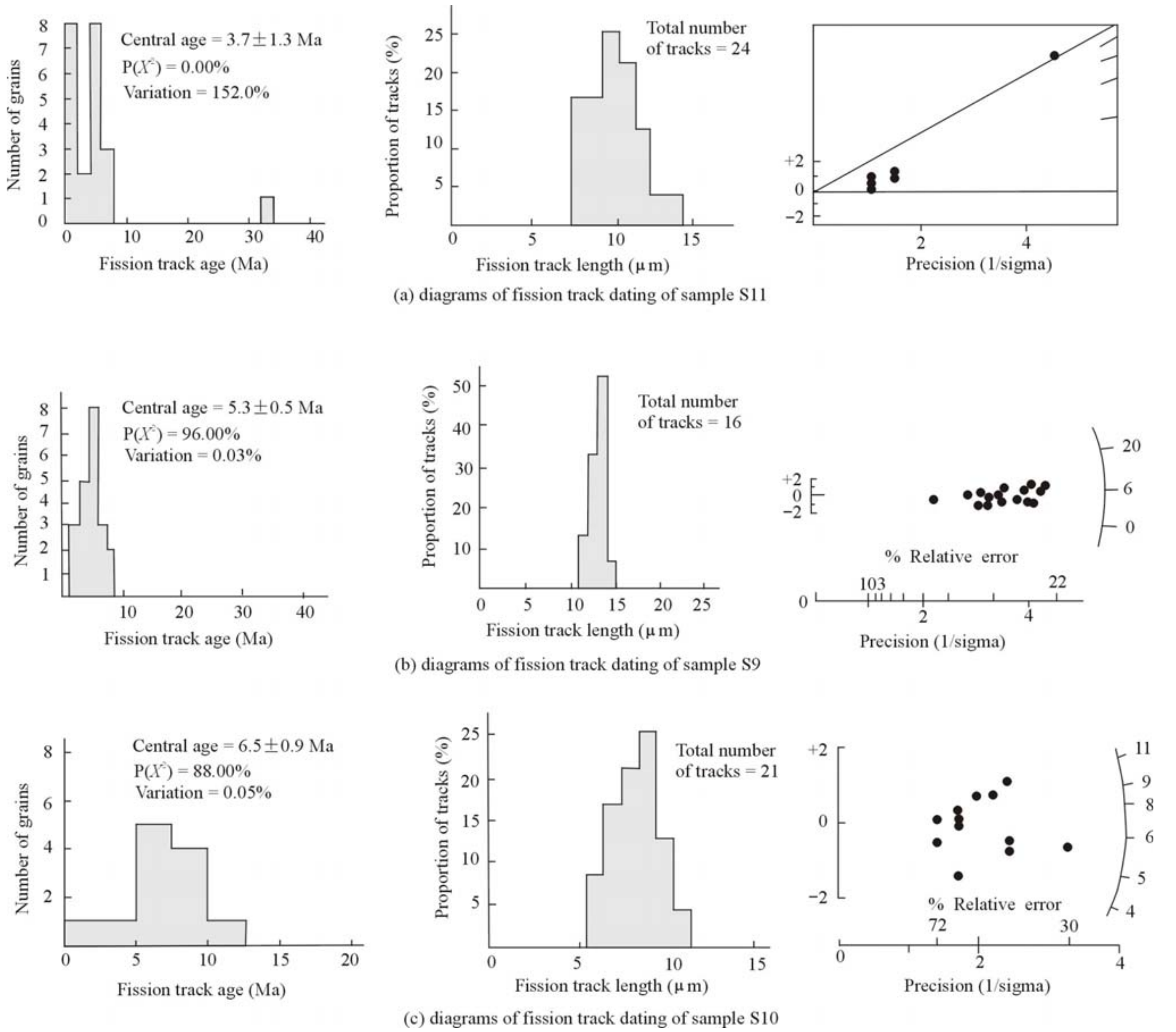

Fig. 8. Diagrams of fission-track dating of apatite from samples adjacent to the Yangbajain basin. (a) and (b), Nyainqêntanglha granite west of the basin; (c) Eocene granite east of the basin.

4.4 $^{40}Ar/^{39}Ar$ dating of time constraints on strike-slip faults

$^{40}Ar/^{39}Ar$ isotopic dating provides some time constraints for dextral strike-slip movement of the Gangdise and Jiali faults. Zhou et al. (2004) reported a 10.8 Ma age for K-feldspar from a granite dike across the Namling-Majiang fault of the Gangdise system north of the Wuyu basin (Table 2, Fig. 1). This suggests that the Namling-Majiang faulting stopped by 10.8 Ma. Volcanic rocks of the Wuyu Group, which are cut by the fault (Figs. 1 and 4b), have

Table 2 Plateau ages of $^{40}Ar/^{39}Ar$ isotopes for dating the strike-slip faults

Tectonic setting	Rock and mineral for $^{40}Ar/^{39}Ar$ dating	Plateau age	Implication	References
East section of the Jiali strike-slip fault	Biotite, K-feldspar and amphibole from mylonite and foliated granite	17.5±0.5 Ma to 11.7±0.1 Ma	Time of dextral shearing and most active phase of the JLF	Lee et al., 2003
Volcanic rock of the Wuyu Group	Feldspar and mica	15.10±0.49 Ma to 14.03±0.37 Ma	Time of volcanic sedimentary strata	Spicer et al., 2003
Dacite and trachite of the Wuyu Group	K-feldspar and plagioclase	12.00±0.13 Ma to 13.63±0.14 Ma	Time of volcanic sedimentary strata	Zhou et al., 2004
Granite vein across the Namling-Majiang fault NW of site 2	K-feldspar from sample GZ6	10.84±0.34 Ma	Terminal time for dextral slip and oblique thrust	Zhou et al., 2004

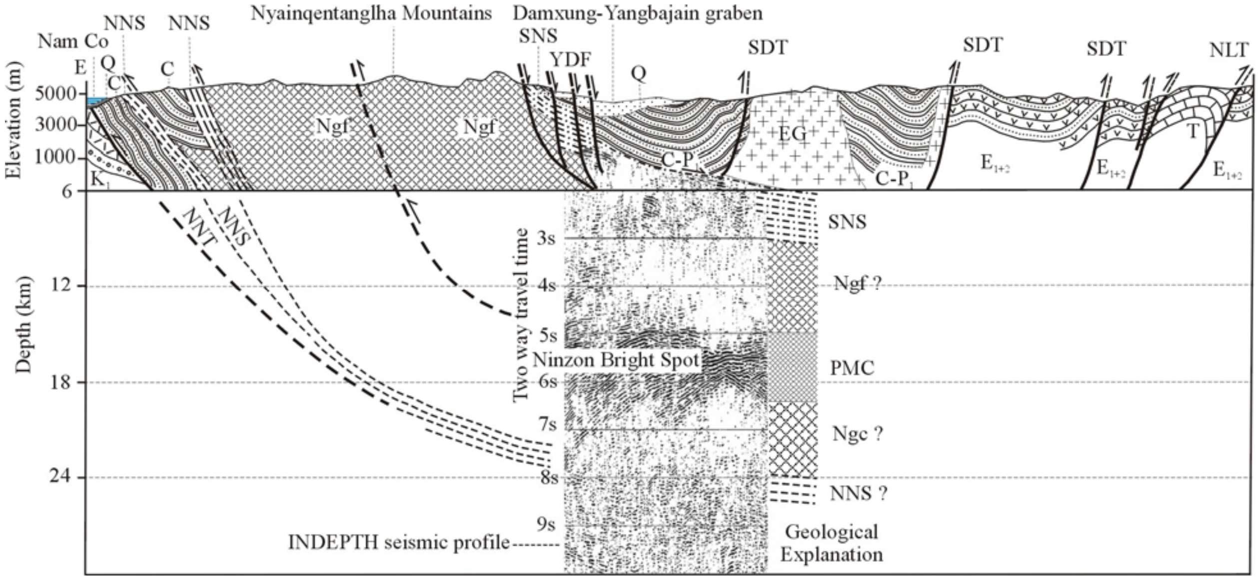

Fig. 9. Cross-section along profile E-F, Fig. 1, across the Nyainqêntanglha Mountains and the Damxung-Yangbajain basin, showing correlation with the INDEPTH seismic reflection profile of Brown et al., 1996.

^{40}Ar/^{39}Ar ages of 12.0–13.6 Ma (Zhou et al., 2004) and 14.0–15.1 Ma (Spicer et al., 2003) (Table 2), which demonstrates that the Namling-Majiang fault was at least active after 12–15 Ma in the Late Miocene. These data fit well with the ^{40}Ar/^{39}Ar ages for dextral shearing of the Jiali fault of 11.7–17.5 Ma as determined by Lee et al. (2003). These dates indicate that dextral-slip, together with oblique-thrust movement of the Gangdise fault system southwest of the Nyainqêntanglha Mountains, occurred in the same period as ductile shearing of the Jiali fault northeast of them. It is further inferred that the main phase of dextral-slip faulting in the Nyainqêntanglha region occurred in ~11–18 Ma during emplacement of the Nyainqêntanglha granite.

5 Depth of Formation of the Nyainqêntanglha Granite

The Nyainqêntanglha batholith was formed as an intermediate-depth syntectonic granite. Geochemical data of the Nyainqêntanglha granite support a genetic relation between the Nyainqêntanglha thrust system and the granite plutonism. Geochemical diagrams of R1 vs. R2 and Rb vs. Y+Nb indicate that the Middle Miocene granites, both fine- and coarse-grained varieties, are of a syn-collisional type (Liu et al., 2004), which is also demonstrated by their flow foliation. This foliation is shown mainly by the alignment of biotite and affects all but the central portion of the granite. The collision related to the granite generation can only be the thrust system as reasonably explained by Fig. 9. Geo-barometer and geo-thermometer data from gneiss pendants within the granite show that the enclosed metamorphic rocks formed under pressure of 0.22–0.46 GPa and temperature of ~500°C–600°C (Table 3), which correspond to depths of 8–17 km by taking the rock density of the upper crust as 2.7g/cm^3 and depths of 14–17 km by taking a geotherm of 35°C/km. These data show that the gneiss trapped in the magma chamber was formed deep in the crust where partial melting occurred, and agree with the possibility that partially melted crust is indicated by the bright spot found at depth in the seismic survey to the east.

The deep seismic reflection profiles of the INDEPTH-II survey along the Damxung-Yangbajain graben provide

Table 3 Temperature and pressure data of the hornblende-plagioclase thermo-barometer of gneiss enclosed in the top of the Nyainqêntanglha granite

Sample	Type of enclosed rocks	XAnPl	XCaHb	∑AlHb	T1 (°C)	T2 (°C)	P (GPa)
P71-2 (1+2)	Biotite-plagioclase schist	0.2953	0.7956	1.346	515	538	0.26
P71-2 (3+4)	Biotite-plagioclase schist	0.324	0.770	1.354	540	545	0.22
P71-3 (1+2)	Amphibole-plagioclase gneiss	0.368	0.742	1.934	590	555	0.42
P71-3 (3+4)	Amphibole-plagioclase gneiss	0.321	0.758	1.702	545	540	0.40
P71-6 (3+4)	Metamorphic granodiorite	0.209	0.601	1.609	570	520	0.46
Average					552	540	0.35

Note: The temperature and pressure of gneiss inclusions were derived from the hornblende-plagioclase balance function by Perchuk (1966), and the related method and test procedure were described by Hu et al., 2004.

high-resolution data to interpret the deep structure of the Nyainqêntanglha region. Brown et al. (1996) and Nelson et al. (1996) discovered bright spots in the records at depths of 13–20 km in the Angan, Yangbajain, Ninzon and Damxung areas and considered them to represent the partially melted crust. Brown et al. (1996) further traced the southeastward extension of the Southeast Nyainqêntanglha shear zone beneath the Damxung-Yangbajain graben. These interpretations, in combination with the field and laboratory data, allow an analysis of the deep structure of the Nyainqêntanglha Mountains.

The shear zone extends gently southeastward beneath the Damxung-Yangbajain graben, where it is offset by normal faults (Brown et al., 1996). The upper crustal section beneath the shear zone has no evident seismic reflection corresponding to granite, but a zone of seismic bright spots apparently due to partially melted crust occurs between depths of 13 to 20 km (Fig. 9). Another seismic survey beneath Ninzon has scattered reflections that seem to be from a deep extension of the Nyainqêntanglha granite, and seismic reflections below ~24 km may be an extension of the North and Northwest Nyainqêntanglha thrust faults (Fig. 9). The agreement of the depth of formation of the granite from temperature and pressure data with that of the seismic data supports the presence of partially melted crust that may possibly be the remains of the magma chamber source for the granite.

6 Tectonic Evolution of the Nyainqêntanglha Region during and after the Miocene

The beginning of the Miocene appears to mark a change in the tectonic movement in central Tibet and the structures developed then cut obliquely across the earlier ones. The Gangdise batholitic complex and other early granite bodies lie in an east-west zone and apparently formed under north-south compression from the movement along the Yarlung Zangbo suture during Late Cretaceous to Eocene. One of the younger of these granites, the Eocene Yangbajain, ranges in ages from 52.5 to 48 Ma east of Yangbajain (Xu et al., 1985; Wu et al., 2003). These granites were subsequently uplifted and probably tilted northward as Eocene deposits, dated at 46.3 to 41.8 Ma near Yangbajain (Wu et al., 2003), overlapped their northern border, while the post-Lower Cretaceous strata may have been stripped off to the south (Fig. 3). This pattern was disrupted in the Miocene by a new set of kinematically related structures and the northeast-trending Nyainqêntanglha granite as the compression alignment shifted to the northwest-southeast.

Dextral-oblique movement resulting from this shift formed a northeast-trending thrust fault in the position of the Nyainqêntanglha Mountains and drove the western Nam Co block downward beneath the eastern Lhasa block. Dextral-slip along the Gangdise fault system was effectively transferred northward along this proto-Nyainqêntanglha thrust to the North Damxung- Jiali zone. This occurred in Early Miocene or slightly earlier (Fig. 10a). The thrust may have been preceded by an initial downwarp that helped trap deposits in the Eocene or soon after, to preserve them, as suggested by the concentration of Eocene strata east of the mountains (Fig. 1). Much of the post-Oligocene and Middle Miocene volcanic rocks, dated at 15 to 12 Ma, appear to be trapped in the Wuyu basin which was formed during dextral-slip movement of the Gangdise fault system. The major phase of dextral shearing of the Jiali fault and dextral-slip and oblique thrust movement of the Gangdise system was during 18.3–11 Ma, when the Nyainqêntanglha syntectonic granite was formed and under-thrust on the northwest to shear the Northwestern Nyainqêntanglha thrust zone along its border at ~12 Ma (Figs. 9 and 10b). The downward movement and friction along the proto-Nyainqêntanglha thrust apparently led to partial melting of the crust and formation of the granite at depths of 12 to 15 km. Granite of the same type was formed along similar deep thrusts in the Northern Appalachian collision zone and continued movement also formed sheared borders (Barosh, 1982, 1991, 2005). The ~50 km distance from the Northwestern Nyainqêntanglha outcrop to the deep seismic section beneath Ninzon to the southeast is close to the total measured dextral-slip of the Gangdise faults (Fig. 1) and may represent the extension of the Nyainqêntanglha thrust system at depth. The average dextral-slip rate of the Gangdise or average southeastward subduction rate of the western Nam Co block is ~7 mm/a in the period of 18–11 Ma; this being equal to or a little more than the relatively northwestward thrust rate of the Nyainqêntanglha thrust system. These consistent data indicate that dextral-oblique-slip along the Gangdise fault system caused the relative southeastward subduction of the Nam Co block beneath the Lhasa block and thereby creating the intervening Nyainqêntanglha batholith. This intracontinental subduction and granite plutonism in the Miocene may have been accompanied by other ductile shear zones, found locally within the adjacent South Damxung, North Lhünzhub, East Yangbajain and Gangdise fault systems, which acted to adjust for the movement to the east and south.

Dextral strike-slip along the Gangdise, North Damxung and Jiali faults greatly slowed or even stopped by ~11 Ma, but continued in dextral shearing of Guren Qu at 12.7–9.8 Ma and followed by shearing along the Southeastern Nyainqêntanglha zone at 8.6–8.3 Ma (Figs. 10c and 11).

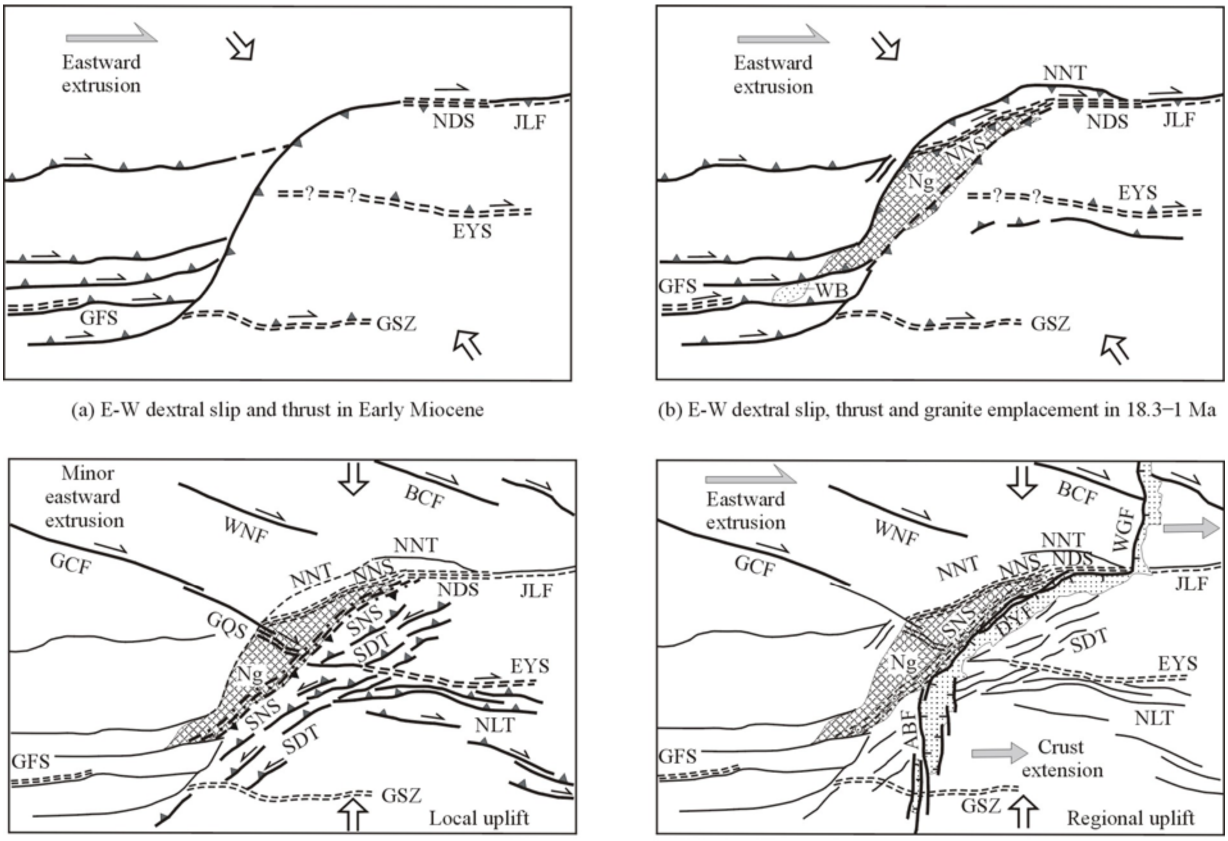

(a) E-W dextral slip and thrust in Early Miocene

(b) E-W dextral slip, thrust and granite emplacement in 18.3−1 Ma

(c) NW dextral-slip, thrust and SNS extensional shear in 11−8.3 Ma

(d) NW destral-slip and normal faulting since 6.5 Ma

Fig. 10. Maps showing the tectonic evolution of the Nyainqêntanglha region since the Oligocene.
(See Fig. 1 for explanation).

Dextral movement of the north-dipping Guren Qu and East Yangbajain zones may represent the start of renewed north-south compression and the beginning of en echelon right-lateral strike-slip movement along the northwest-trending faults of the Karakorum-Jiali system in southern Tibet. This system of en echelon faults lies to the northwest of the Nyainqêntanglha Mountains in the Nam Co block, whereas the system of northeast-trending left-lateral thrust faults of the South Damxung system are found to the southeast in the Lhasa block (Fig. 1). Taken together they suggest that the north-south compression acted differently on both sides of the Nyainqêntanglha batholith. The South Damxung system itself is replaced farther east by west-northwest-trending, north-dipping dextral-slip thrust faults of the North Lhünzhub system. The initial rise of the Nyainqêntanglha batholith under the north-south compression can account for these geographic differences in the fault pattern. A rising batholith would produce a southeastward slope that added a gravity component to the compression, to result in thrusting to the southeast instead of strike-slip faults. The dextral strike-slip component again appeared to the east away from the slope. This uplift is also marked by the change from the earlier ductile faults to brittle ones. The uplift and arching over the southeast-dipping batholith would be concentrated along its southeast side and could have possibly stretched the uplifted rock to account for the minor indications of down-to-the-southeast offset along the gently southeast-dipping shears or they are simply due to gravitational back-sliding. In any case, this movement along the Southeast Nyainqêntanglha zone occurred about 8.6–8.2 Ma in the Late Miocene (Fig. 10c) and would mark the time of the uplift. The uplift of the batholith appears to be due to the cessation of the right-lateral movement that helped create it and the buoying upward of the thickened crust.

Regional crustal extension began near the end of the Miocene, ~6.5 Ma (Figs. 10d and 11), and initiated the Damxung-Yangbajain, Gulu and Angan grabens and their attendant bordering normal fault zones; an extension that accelerated in the Quaternary at ≤5.3 Ma, (Fig. 10d). This Quaternary extension is well documented by offset structures of the Miocene structural systems and Quaternary deposits of the grabens (Yin et al., 1999). Such grabens form cross structures (Wu et al., 1998) that are distributed widely across the southern Tibetan Plateau (Amijo et al., 1986). Here the extension forming the cross structures of the Gulu and Angan grabens is connected by

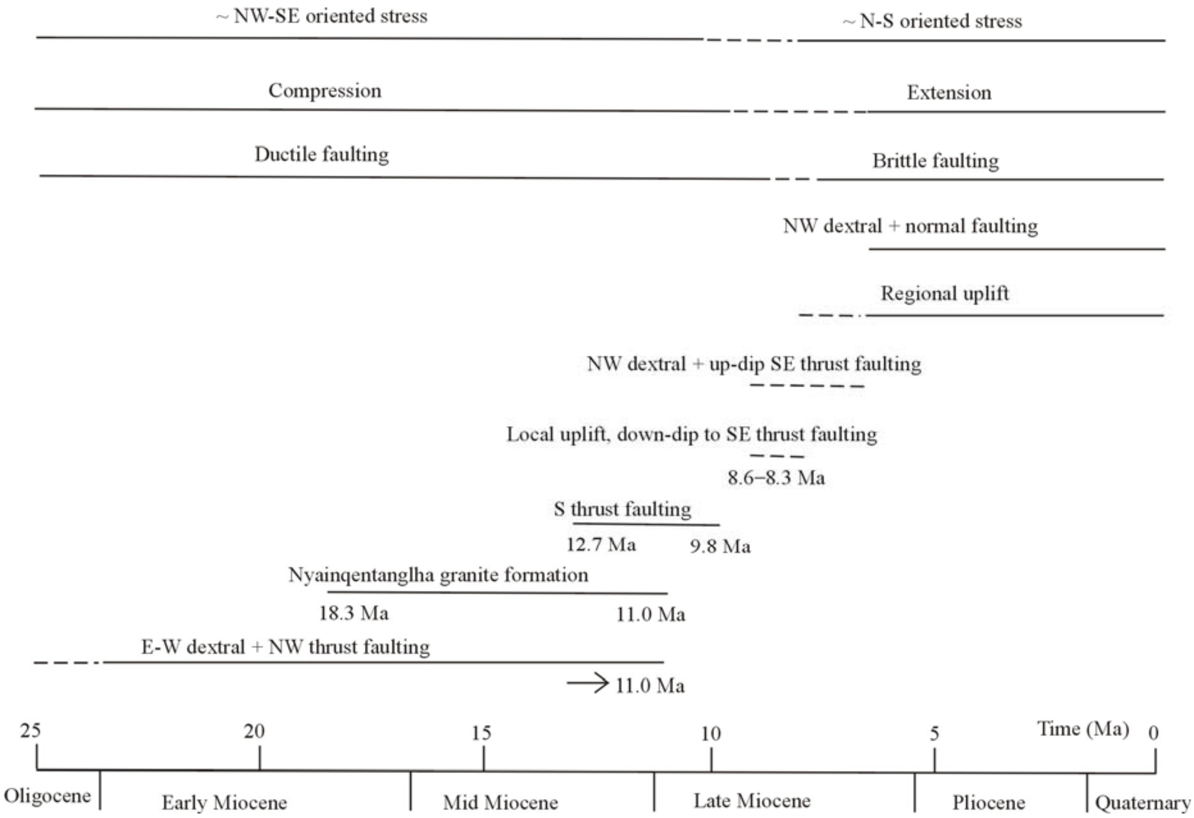

Fig. 11. Diagram showing the time of post-Oligocene tectonic movements in the Nyainqêntanglha region.

the Damxung-Yangbajain graben, which is closely controlled by the earlier Miocene structures along the southeastern side of the Nyainqêntanglha uplift and serves to transfer the extension between the north-trending grabens. The vertical slip rates of the Damxung-Yangbajain and West Gulu border faults are almost equal to the uplift rate of the Nyainqêntanglha Mountains in the Pleistocene (Fig. 7), and demonstrate how well the normal faulting is coupled with the uplift. An uplift might possibly still contain a small component due to the granite rising. The extension northwest of the mountains is adjusted by the continued movement along the Karakorum-Jiali fault system. This system and the grabens remain very active at present.

7 Conclusion and Discussion

Three main phases of faulting occurred in the Nyainqêntanglha region during the Miocene and recorded a change from compression to extension (Fig. 11). Connected systems of dextral-slip faults and thrust faults developed across the region by the Early Miocene. Their movement, under northwest-southeast aligned compression, drove the western side relatively southeastward beneath the position of the Nyainqêntanglha Mountains and generated a granitic batholith in the Mid-Miocene. The cessation of this movement resulted in a buoyed uplift of the batholith in the Late Miocene under a north-south compression. This developed a local stress barrier separating the northwest-trending dextral-slip faults northwest of the batholith from the northeast-trending sinistral-slip thrust faults adjacent to its southeastern side and the dextral-slip west-northwest-trending thrust faults farther to the east. Near the end of the Miocene a regional uplift developed a north-trending graben system east of the batholith, where the control by earlier faults caused a local deviation to the northeast. These grabens and the northwest-trending faults remain very active.

The timing of the elevation of the Tibetan plateau has been regarded as the transition of the tectonic movement from thrusting to extension (Dewey et al., 1988). Harrison et al. (1995) took the initial age of the down-dip shearing on the Southeastern Nyainqêntanglha shear zone, ~8 Ma, as the time the southern Tibetan Plateau rose to its present elevation and Blisniuk et al. (2001) took the initial age of mica from the normal boundary fault of the Shuanghu graben, ~13.5 Ma, as the time of uplift of the northern Tibetan Plateau to its present elevation. However, the tectonic process is found to be more complicated. The down-dip movement along the shear zone is only a local feature along the southeast margin of the Nyainqêntanglha batholith and the fault is clearly different from the normal faults and regional crustal extension indicated by the Gulu, Damxung-Yangbajain and Angan grabens. This down-dip movement fits with back-sliding or stretching during the uplift of the batholith. But the latter is a local uplift that infers little about the time of the regional uplift of the southern Tibetan Plateau. This local uplift began after the cessation of the dextral-slip along the Gangdise fault system and the end of thrusting along the Nyainqêntanglha system in ~11 Ma and apparently was underway during the last movement affecting the Southeast shear zone at ~8 Ma. The local nature of the uplift seems responsible for the change in fault pattern across the batholith and the preservation of Eocene and Miocene strata adjacent to the granite that has risen from the depth. The subsequent regional uplift of the Nyainqêntanglha Mountains associated with the development of the widespread graben system is a better indicator of the rise of the southern Tibetan Plateau. This system cuts across the earlier uplift of the Nyainqêntanglha batholith, at the position of the Gulu graben, and demonstrates, at least here, that the regional uplift associated with the grabens is later. The grabens formed at ~6.5 Ma, apparently after the regional rise of the plateau, as subsequent uplift remained in equilibrium with the normal faulting, to judge from the Pleistocene data. Thus, the uplift of the southern Tibetan Plateau to its present elevation appears to have occurred between ~8 Ma and ~6.5 Ma.

Acknowledgements

This study was financially supported by China Geological Survey and the Ministry of Science and Technology of China under grants DKD9901001 and 2001CB711001, respectively. P. J. Barosh gratefully acknowledges the support provided by the Chinese Academy of Geological Sciences through the Institute of Geomechanics.

Manuscript received Jan. 11, 2007
accepted April 1, 2007
edited by Zhu Xiling

References

Amijo, R., Tapponnier, P., Mercier, J.L., and Han, T., 1986. Quaternary extension in south Tibet; field observations and tectonic implications. *J. Geophys. Res.*, 91: 13803–13872.

Armijo, R., Tapponnier, P., and Han, T., 1989. Late Cenozoic right-lateral strike-slip faulting in southern Tibet. *J. Geophys. Res.*, 94: 2787–2838.

Barosh, P.J., 1982. Structural relations at the junction of the Merrimack Province, Nashoba Thrust Belt and Southeast New England Platform in the Webster-Oxford area, Massachusetts, Connecticut and Rhode Island. In: Barosh, P.J. (ed.), *Connnecticut State Geological and Natural History Survey, Guidebook*. 5: 395–418.

Barosh, P.J., 1991. Regional geologic setting of Boston. In: Woodhouse, D., and Barosh, P.J. (eds.), Geology of Boston, Massachusetts, United States of America. *Bulletin of Association of Engineering Geologists and Massachusetts Geological Survey*, 28: 386–408.

Barosh, P.J., 2005. *Geology of the Oxford Quadrangle, Massachusetts, Connecticut and Rhode Island*. Massachusetts Geological Survey, scale 1: 24,000.

Blisniuk, M.P., Bradley, R.H., Glodny, J., Ratschbacher, L., Bi, S., Wu, Z., McWilliams, O.M., and Calvert A., 2001. Normal faulting in central Tibet since at least 13.5 Ma ago. *Nature*, 412: 628–632

Brown, L.D., Zhao, W., Nelson, K.D., Hauck, M., Alsdorf, D., Ross, A., Cogan, M., Clark, M., Liu, X., and Che, J., 1996. Bright spots, structure and magmatism in southern Tibet from INDEPTH seismic reflection profiling. *Science*, 274: 1688–1690.

Chen Leshou, Booker R. J., Jones G. A., Wu, N., Unsworth J. M., Wei W., and Tan, H., 1996. Electrically conductive crust in Southern Tibet from INDEPTH magnetotelluric surveying. *Science*, 274: 1694–1696.

Cheng Liren, Wang Tianwu, Li Cai, Wu Shizhong, Zhao Juncai, He Zhonghua, Zhang Yujie, Zhu Zhiyong and Yang Deming, 2003. *Report of Regional Geological Survey of Xainza Area with Attachment of Geologic Map at Scale 1:250000*. Beijing: China Geological Survey, 247 (in Chinese).

Copeland, P., Harrison, T.M., Pan, Y., Kidd, W.S.F., and Roden, M., 1995. Thermal evolution of the Gangdise batholith, southern Tibet: a history of episodic unroofing. *Tectonics*, 14 (2): 223–236.

Dewey, J.F., Shackleton, R.M., Chang Chengfa and Sun Yiyin, 1988. The tectonic evolution of the Tibetan Plateau. *Royal Society of London Philosophical Transaction*, Series A, 327: 379–413.

Geology Institute of China Seismological Bureau, 1992. *Active Faults in Central Tibet*. Beijing: Seismic Press, 31–104 (in Chinese).

Gleadow, A.J.W., and Duddy, I.R., 1981. A natural long-term annealing experiment for apatite. *Nuclear Tracks and Radiate Measurement*, 5: 169–174.

Harrison, T.M., Copeland, P., Kidd, W.S.F. and An, Y., 1992. Raising Tibet. *Science*, 225: 1663–1670.

Harrison, T.M., Copeland, P., Kidd, W.S.F., and Lovera, O.M., 1995. Activation of the Nyainqêntanghla shear zone: Implications for uplift of the southern Tibetan Plateau. *Tectonics*, 14: 658–676.

Harrison, T.M., Pan Y., Kidd, W.S.F., and Roden, M., 1995. Thermal evolution of the Gangdise batholith, southern Tibet: A history of episodic unroofing. *Tectonics*, 14: 223–236.

Hu Minren, Nima Ciren, Fan Yuecheng, Chen Guojie, Liu Wenrui and Sun Zhongliang, 2003. *Report of Regional Geological Survey of Xigazê Area with Attachment of Geologic Map at Scale 1:250000*. Beijing: China Geological Survey, 182 (in Chinese).

Hu Daogong, Wu Zhenhan, Jiang Wan and Ye Peisheng, 2004. P-T-t path of mafic granulite metamorphism in northern Tibet and its geodynamical implications. *Acta Geologica Sinica* (English edition), 78(1): 155–165.

Hurford, A.J.W., and Green, P.F., 1982. The zeta age calibration of fission-track dating. *Chem Geol*, 1: 285–317.

Kapp, J.L.D., Harrison, T.M., Kapp, P., Grove, M., Lovera, O.M., and Ding, L., 2005. Nyainqêntanglha Shan: A window into tectonic, thermal, and geochemical evolution of the Lhasa block, southern Tibet. *J. Geophys. Res.*, 110, B08413, doi 10.1029/2004JB00330

Kidd, W.S.F., Pan, Y., Chang, C., Coward, M.P., Dewey, J. F., Gansser, A., Molnar, P., Shackleton, R. M., and Sun, Y., 1988. Geological mapping of the 1985 Chinese-British Tibetan (Xizang-Qinghai) Plateau geotraverse route. *Royal Society of London Philosophical Transaction*, Series A, 327: 287–305.

Lee, H., Chung, S., Wang, J., Wen, D., Lo, C., Yang, T.F., Zhang, Y., Xie, Y., Lee, T., Wu, G., and Ji, J., 2003. Miocene Jiali faulting and its implications for Tibetan tectonic evolution. *Earth Planet. Sci. Lett.*, 205: 185–194.

Li Dinghong, Xu Guozhang et al., 1993. *Report of Regional Geological Survey of Lhasa Area with Attachment of Geologic Map at Scale 1:200000.* Lhasa: Tibeten Bureau of Geology and Mineral Resources, 124 (in Chinese).

Liu Qisheng, Wu Zhenhan, Hu Daogong, Ye Peisheng, Jiang Wan, Wang Yanbing and Zhang Hancheng, 2004. SHRIMP U-Pb zircon dating on Nyainqêntanglha granite in central Lhasa block. *Chinese Sci. Bull.*, 49(1): 76–82.

Nelson, K.D., Zhao, W., Brown, L.D., Kuo, J., Che, J., Liu, X., and Klemperer, S.L., 1996. Partially molten middle crust beneath southern Tibet: Synthesis of Project INDEPTH results. *Science*, 174: 1684–1688.

Pan, Y., and Kidd, W.S.F., 1992. Nyainqêntanglha shear zone: A late Miocene extensional detachment in the southern Tibetan plateau. *Geology*，22: 775–778.

Pan Guitang, Ding Jun, Yao Dongsheng, Wang Liquan et al. (eds.), 2004. *Geological Map of the Tibetan Plateau and Its Adjacent Areas at Scale 1:1500000*. Chengdu: Chengdu Map Press.

Perchuk, L.L., 1966. Coefficiency of temperature on Ca equilibrium between plagioclase and amphibole. *Transaction of USSR Academy of Sciences*, 60 (6): 1436–1438.

Spicer, R.A., Harris, N.B.W., Widdowson, M., Herman, A.B., Guo, S., Valdes, P.J., Wolfe, J.A., and Kelley, S., 2003. Constant elevation of southern Tibet over the past 15 Million years. *Nature*, 421: 622–624.

Tapponnier, P., Peltzer, G., and Armijo, R., 1986. On the mechanism of the collision between India and Asia. In: Coward, M.P., and Ries, A.C. (eds.), *Collision Tectonics*. Geological Society Special Publication, 19: 115–157.

Tapponnier, P., Xu, Z., Roger, F., Meyer, B., Arnaud, N., Wittlinger, G., and Yang, J., 2001. Oblique stepwise rise and growth of the Tibetan Plateau. *Science*, 294: 1671–1677.

Tibet Bureau of Geology and Mineral Resources, 1993. *Geology of Tibet Autonomous Region with Attachment of Geological Map at Scale 1:1500000*. Beijing: Geological Publishing House, 566.

Wagner, G.A., and Van den haute, P., 1992. *Fission-Track Dating.* Dordrecht: Kluwer Academic Publisher, 145–158.

Wagner, G.A., 1998. *Age Determination of Young Rocks and Artifacts*. Berlin: Springer-Verlag, 219–294.

Wu Zhenhan, Meng Xiangang, Hu Daogong, Jiang Wan, Ye Peisheng, Zhu Dagang, Liu Qisheng, Yang Xinde, Shao Zhaogang, Wu Zhonghai et al., 2003. *Report of Regional Geological Survey of Damxung Area with Attachment of Geologic Map at Scale 1:250000.* Beijing: China Geological Survey, 618 (in Chinese).

Wu Zhenhan, Hu Daogong, Ye Peisheng, Zhao Xun and Liu Qisheng, 2004a. Thrusting of the North Lhasa Block in the Tibetan Plateau. *Acta Geologica Sinica* (English edition), 78 (1): 246–259.

Wu Zhenhan, Hu Daogong, Wu Zhonghai et al., 2005. *Active Faults and Geological Hazards along the Golmud-Lhasa Railway across the Tibetan Plateau*. Beijing: Geological Publishing House, 383 (in Chinese with English abstract).

Wu Zhonghai, Zhao Xitao, Wu Zhenhan, Jiang Wan, Hu Daogong and Zhou Chunjing, 2004b. Quaternary geology and faulting in the Damxung-Yangbajain basin. *Acta Geologica Sinica* (English edition), 78(1): 273–282.

Wu, C., Nelson, K.D., Wortman, G., Samson, S.C., Li, J., Kidd, W.S.F., and Edwards, M.A., 1998. Yadong cross structure and south Tibetan detachment in the east central Himalaya. *Tectonics*, 17: 28–45.

Xu, R.H., Scharer, U., and Allegre C.J., 1985. Magmatism and metamorphism in the Lhasa block (Tibet): A geochronological study. *J. Geol.*, 93: 41–57.

Yin, A., Harrison, T.M., Reyerson F.J., Chen, W., Kidd, W.S.F., and Copeland, P., 1994. Tertiary structural evolution of the Gangdise thrust system in southern Tibet. *J. Geophys. Res.*, 99: 18175–18201.

Yin, A., Kapp, P.A., Murphy, M.A., and others, 1999. Evidence for significant late Cenozoic east-west extension in north Tibet. *Geology*, 27: 787–790.

Yin, A., and Harrison, T.M., 2000. Geologic evolution of the Himalayan-Tibetan orogen. *Earth Planet. Sci. Lett.*, 28: 211–280.

Zhang Jianmin, Luo Fengcai et al., 1994. *Report of Regional Geological Survey of Quxi Area with Attachment of Geologic Map at Scale 1:200000*. Lhasa: Tibet Bureau of Geology and Mineral Resources, 156 (in Chinese).

Zhou Su, Mo Xuanxue, Zhao Zidan, Qiu Ruizhao, Zhang Shuangquan and Guo Tieyin, 2004. $^{40}Ar/^{39}Ar$ isotopic dating of volcanic rocks of the Wuyu basin in Namling County of Tibetan Autonomous Region. *Symposium of Petrology and Geodynamics of China in 2004, Haikou*: 413–416 (in Chinese).

Zhao, W., Nelson, K.D., and Project INDEPTH Team, 1993. Deep seismic reflection evidence for continental underthrusting beneath southern Tibet. *Nature*, 366: 557–559.